Supplemental Material for :

How Can a Single Second Sphere Amino Acid Substitution Cause Reduction Midpoint Potential Changes of Hundreds of Millivolts ?

Emine Yikilmaz, Jason Porta, Laurie E. Grove, Ardeschir Vahedi-Faridi, Yuriy Bronshteyn, Thomas C. Brunold, Gloria E. O. Borgstahl, and Anne-Frances Miller *

Production of proteins:

Mutant versions of the FeSOD gene were constructed from the WT gene using the megaprimer method,[1] and were confirmed to contain only the desired mutation by restriction analysis (AatII, XhoI, XbaI) and sequencing of both DNA strands. The resulting plasmids (derivatives of pET21) were each transformed into the DE3 lysogen of the *sodA*$^-$/*sodB*$^-$ strain of *E. coli*, QC774.[2] Cultures were grown in LB or minimal medium supplemented with ampicillin and kanamycin (50 μg/ml each), and protein expression was induced by addition of 0.1-0.4 mM IPTG (Isopropyl β-D-thiogalactopyranoside), as well as 0.1 mM $FeCl_3$, when the optical density at 600 nm reached 1. Cells were harvested four hours later, and the protein was purified as described by Sorkin and Miller[3] and Slykhouse and Fee[4].

Energetic consequences of a local Glu residue serving as donor of a redox-coupled proton, instead of a local water molecule.

If the proton to be acquired in a proton-coupled electron transfer reaction is to be drawn from a local weak acid 'AH', we can assign this group an acid dissociation constant K_A. We also denote the acid dissociation constant of Fe^{2+}-coordinated solvent by K_{red}. In this we refer to the oxidized Fe site including the coordinated OH^- as 'Ox' and the reduced Fe side including the coordinated H_2O as 'RedH'. (Our data support coordinated H_2O in the mutant reduced state based on the WT-like NMR spectrum and the Fe-O crystallographic distance. The EPR of Q69E-Fe^{3+}SOD suggests coordination of an additional exogenous anion thereby implying that the existing solvent has already ionized.) Thus we have:

$$\begin{array}{cccc} & & E_{m,Htet} & \\ & Ox + e^- + AH & \Leftrightarrow & RedH + A^- \\ K_A & \uparrow\downarrow & & \uparrow\downarrow \quad K_{red} \\ & Ox + e^- + A^- + H^+ & \Leftrightarrow & Red^- + H^+ + A^- \\ & & E_m & \end{array}$$

Where E_m is the reduction midpoint potential of $Ox + e^- \Leftrightarrow Red^-$ alone and $E_{m,Htet}$ is the proton-coupled electron transfer reduction potential of $Ox + e^- + AH \Leftrightarrow RedH + A^-$.

By summing the energies associated with the three sides of the box annotated in blue (K_A, E_m and K_{red}), we can evaluate the energy associated with the top reaction, in red ($E_{m,Htet}$).

Thus $-FE_{m,Htet} = -RT \ln (K_A) - FE_m + RT \ln(K_{red})$

so $E_{m,Htet} = E_m + RT/F \ln(K_A/K_{red}) = E_m - 2.3RT/F\ (pK_A - pK_{red})$.

We now compare this $E_{m,Htet}$ for two cases, one in which AH is water (pK_{H2O} =15.7) and one in which AH is Glu (pK_{Glu} = 4.3).

In the case of water serving as the local proton source (A local molecule of water is observed in the channel next to the active site in all SOD crystal structures solved so far.)

$E_{m,H2O} = E_m - 2.3RT/F\ (pK_{H2O} - pK_{red})$.

In the case of Glu as the local proton source we have

$E_{m,Glu} = E_m - 2.3RT/F\ (pK_{Glu} - pK_{red})$.

Thus

$E_{m,Glu} - E_{m,H2O} = -2.3RT/F\ (pK_{Glu} - pK_{H2O}) = 2.3RT/F\ (pK_{H2O} - pK_{Glu})$

≈ 60 mV * (15.7 - 4.3) $\approx$ **680 mV**

IF we assign Glu69 a pK typical of a solvated Glu side chain.

We note however that a pK of 4.3 cannot be a good assumption for Glu69 in Fe^{3+}SOD, as Q69E-Fe^{3+}SOD's high affinity for an exogenous anion argues that Glu69 is protonated at neutral pH. Thus pK_{Glu} is higher than 8 and the increase based on pK values alone should be significantly less than 680 mV. However, the cost of elevating Glu69's oxidized-state pK enough that Glu69 is protonated will detract from the stability of the oxidized state, thus increasing the E_m, in effect raising the above contribution back up toward 680mV.

At least two other factors are also involved. The instability of this protonated Glu is clearly mitigated by coordination of an exogenous anion. This specific stabilization of the oxidized state constitutes lowering of E_m. Finally, the pKs of coordinated solvent could be higher in Q69E-Fe^{3+}SOD than in WT-Fe^{3+}SOD, since even neutral Glu69 can only donate *one* H-bond to coordinated OH^- and Tyr34, whereas Gln69 can donate separate H-bonds to both. Therefore, in our model, Glu69 may be less able to stabilize the coordinated OH^- associated with the oxidized state, elevating E_m in Q69E-FeSOD.

Thus, we have (at least) four factors we cannot properly account for that will tend to mitigate one another, but to unknown extents. Therefore, we limit ourselves to a conservative estimate that some **half** of the possible advantage of transferring a proton from Glu instead of water persists: **≈ 340 mV**.

We emphasize that we do not intend these calculations as a means of obtaining the right number for E_m, but simply as a means of evaluating the tenability of our hypothesis: that a change in E_m as large as we observe might be explained by changes in the energetics of proton transfer coupled to electron transfer and related H-bonding.

Table S1 Crystal structure refinement statistics.

A. Contents of model	
Protein	4 x 192 amino acid residues
Dual conformers	77
Iron	4
Coordinated solvent	4
Water molecules	1144
B. Geometry	
r.m.s.d. bonds (Å)	0.007
r.m.s.d. angles (deg.)	1.067
C. X-ray data (%)	
R-factor (30-1.1 Å)	15.9
Free R-factor (5%; 30-1.1 Å)	17.4
D. Average isotropic B-factors (Å^2)	
Protein	12.1 (3.5)[a]
A, B C, D	11.4 (3.8), 10.8 (3.0), 12.8 (3.1), 13.5 (3.4)
Iron	7.8 (1.1)
A, B, C, D	6.8, 7.2, 9.1, 8.5
Hydroxide Ligands	9.2 (1.0)
A, B, C, D	8.6, 8.2, 10.5, 9.3
Solvent	23.5 (7.1)

[a] standard deviations are in parentheses

Table S2. The effect of the assumed ionization state of Glu69 on crystallographic active site bond lengths and hydrogen bond distances (in Å).[a]

A. Covalent bonds (Å)	Q69E-Fe^{2+}SOD neutral Glu69 (2NYB.pdb).[a]	Q69E-Fe^{2+}SOD anionic Glu69
Fe – $N^{\varepsilon 2}_{His26}$	2.20 (0.01)	2.18 (0.02)
Fe – $N^{\varepsilon 2}_{His73}$	2.11 (0.02)	2.11 (0.01)
Fe – $O^{\delta 2}_{Asp156}$	1.92 (0.01)	1.93 (0.02)
Fe – $N^{\varepsilon 2}_{His160}$	2.13 (0.01)	2.12 (0.01)
Fe – $O_{CoordSolv}$[b]	2.16 (0.02)	2.18 (0.01)
B. Hydrogen bonds (Å)		
$O_{CoordSolv}$ • $O^{\delta 1}_{Asp156}$	3.19 (0.02)	3.19 (0.02)
$O_{CoordSolv}$ • $O^{\varepsilon 2}_{Glu69}$	2.78 (0.01)	2.80 (.004)
$O^{\varepsilon 2}_{Glu69}$ • O^{ζ}_{Tyr34}	2.78 (0.04)	2.78 (0.04)
$O^{\varepsilon 1}_{Glu69}$ • $N^{\delta 2}_{Asn72}$	3.16 (0.06)	3.15 (0.05)
$O^{\varepsilon 1}_{Glu69}$ • $N^{\varepsilon 1}_{Trp122}$	2.85 (0.03)	2.85 (0.03)

[a] Average values were calculated over the four monomers in the asymmetric unit, standard deviations are enclosed by parentheses

[b] Coordinated solvent was modeled using atomic scattering factors for O. The methods used to refine the structure did not include any use of charge for this group.

Table S3. Structural parameters for Q69E Fe^{2+}SOD QM/MM geometry-optimized and restrained active sites.

Q69E-Fe^{2+}SOD active site	Crystal Structure	ADF optimized			Partial Opt, restrained bonds
	Experiment (1.1 Å resol[n])	Coord H_2O Glu69- Tyr34H	Coord H_2O [a] Glu69H Tyr34-	Coord. OH^- [b] Glu69H Tyr34H	Coord. OH- [c] Glu69H Tyr34H
Bond lengths (Å)					
$Fe-O_{CoordSolv}$	2.16 (0.02)	**2.266**	**2.266**	**2.269**	**2.335**
$Fe-O^{\delta 2}_{Asp156}$	1.92 (0.02)	1.939	1.939	1.939	1.939
$Fe-N^{\varepsilon 2}_{His26}$	2.20 (0.01)	2.160	2.160	2.160	2.160
$Fe-N^{\varepsilon 2}_{His160}$	2.13 (0.01)	2.101	2.101	2.101	2.101
$Fe-N^{\varepsilon 2}_{His73}$	2.11 (0.02)	2.164	2.164	2.164	2.164
$O_{CoordSolv}-H_{(H\text{-bonds Asp156})}$	--	**0.982**	**0.983**	**0.982**	**0.980**
$O_{CoordSolv}-H_{(H\text{-bonds Glu69})}$	--	**1.014**	**1.012**	**1.014**	**1.418**[c]
$O^{\zeta}_{Tyr34}-H$	--	**1.025**	**1.027**	**1.025**	**1.030**
$C^{\delta}_{Glu69}-O^{\varepsilon 1}_{(H\text{-bonds W122})}$	1.24 (0.02)	1.256	1.254	1.254	1.234
$C^{\delta}_{Glu69}-O^{\varepsilon 2}_{(H\text{-bonds Y34})}$	1.30 (0.01)	1.316	1.316	1.317	1.351
H-bond distances (Å)					
$O^{\varepsilon 2}_{Glu69} \bullet\bullet\bullet O_{CoordSolv}$	2.784 (0.009)	**2.695**	**2.712**	**2.686**	2.431
$H_{CoordSolv} \bullet\bullet\bullet O^{\varepsilon 2}_{Glu69}$		**1.710**	**1.735**	**1.700**	1.418
$H_{CoordSolv} \bullet\bullet\bullet O^{\delta 1}_{Asp156}$		**2.632**	**2.615**	**2.652**	2.940
$H_{CoordSolv} \bullet\bullet\bullet O^{\zeta}_{Tyr34}$		**3.518**	**3.536**	**3.501**	3.744
$O_{CoordSolv} \bullet\bullet\bullet O^{\delta 1}_{Asp156}$	3.19 (0.02)	**3.449**	**3.440**	**3.465**	2.593
$O^{\varepsilon 2}_{Glu69} \bullet\bullet\bullet O^{\zeta}_{Tyr34}$	2.78 (0.04)	**2.645**	**2.641**	**2.643**	2.923
$O^{\varepsilon 1}_{Glu69} \bullet\bullet\bullet N^{\varepsilon 1}_{Trp122}$	2.85 (0.03)	**2.925**	**2.929**	**2.923**	128.0

[a] After geometry optimization, this species is really Fe^{2+}SOD (Glu69$^-$, Tyr-OH with coordinated H_2O) and thus documents proton transfer from Glu69 to Tyr34.

[b] After geometry optimization, this species is really Fe^{2+}SOD (Glu69$^-$, Tyr-OH with coordinated H_2O) and thus documents proton transfer from Glu69 to coordinated solvent.

[c] Proton transfer was prevented by restraining the O-H bond of the Glu69 side chain to 1.051 Å, and those of the Tyr34 side chain and coordinated solvent during geometry optimization. Restrained bonds are indicated in red. Thus, coordinated solvent has only one proton at the end of the calculation.

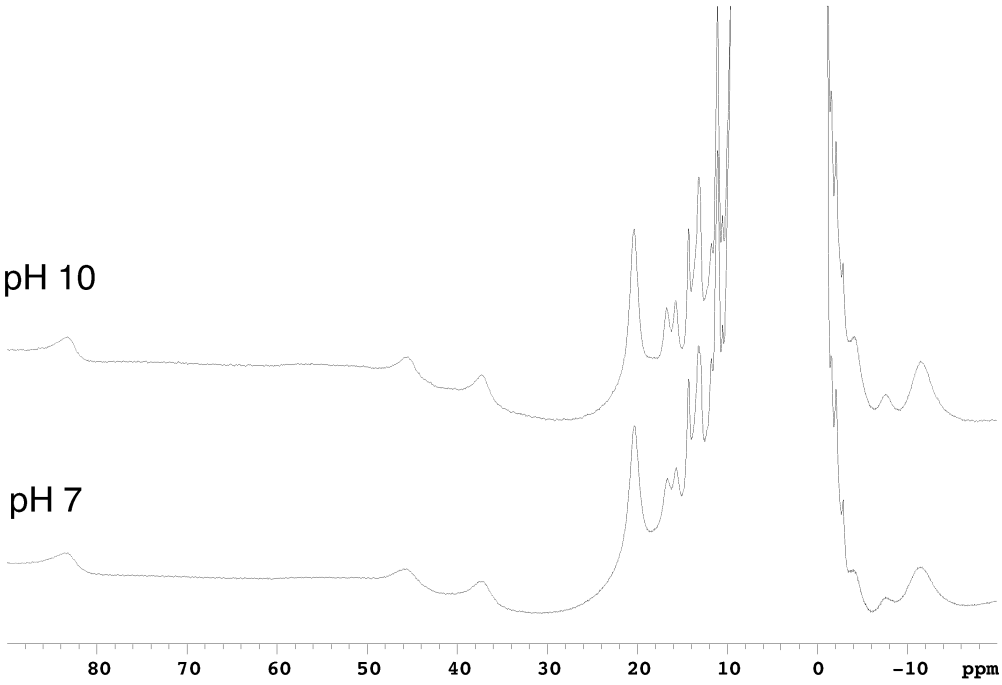

Figure S1. Comparison of NMR spectra of active site residues of Q69E-Fe^{2+}SOD at high and neutral pH, demonstrating the lack of sensitivity to pH in this range.

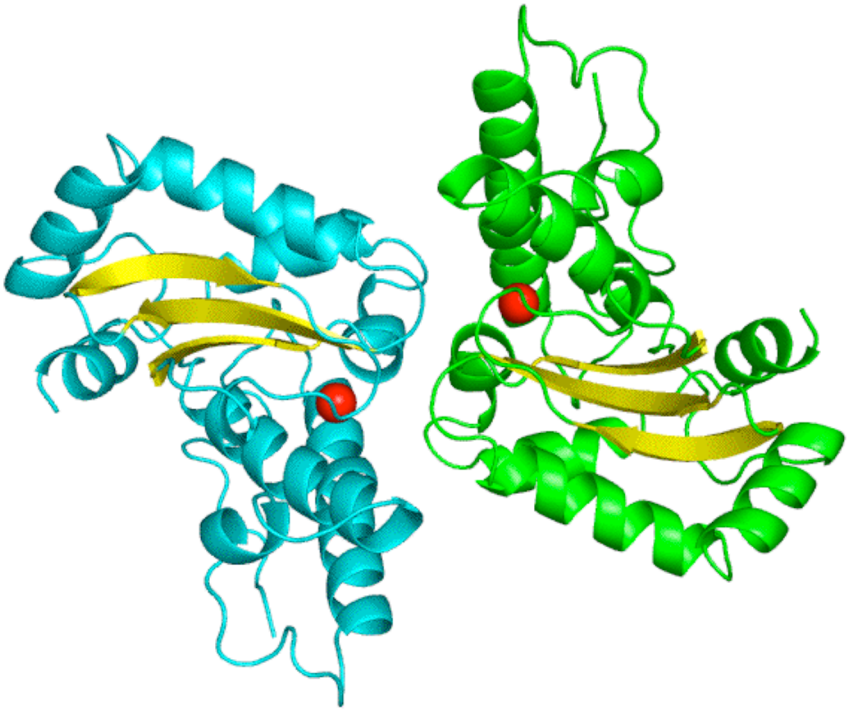

Figure S2: ribbon diagram of Q69E-FeSOD, based on the new structure reported here.

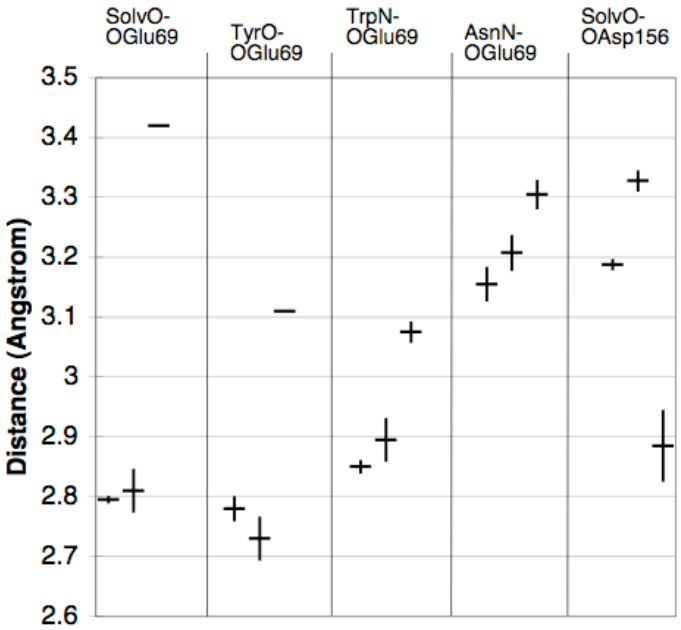

Figure S3: Average H-bond distances (horizontal) and standard deviation (vertical) for Q69E at 1.1 Å (left), Q69E at 1.6 Å (centre) and WT-Fe^{2+}SOD at 1.8 Å (right), respectively, for each bond (separated columns).

Figure S4

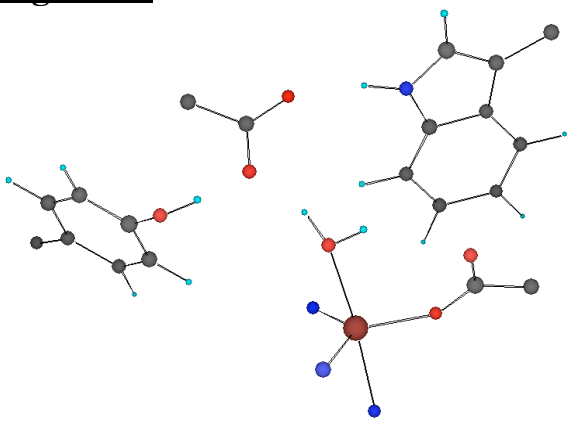

Q69E Fe^{2+}SOD: Coord H_2O, Glu69$^-$, Tyr34H

INPUT GEOMETRY

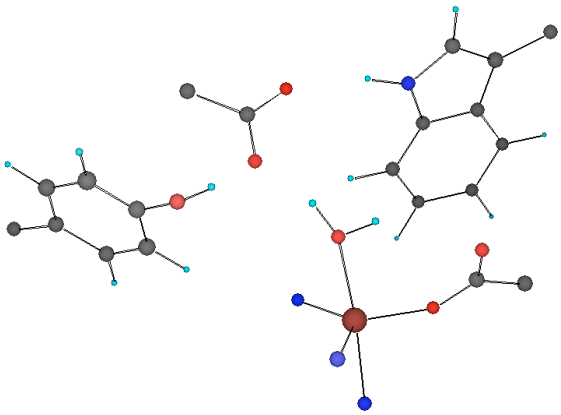

OPTIMIZED GEOMETRY

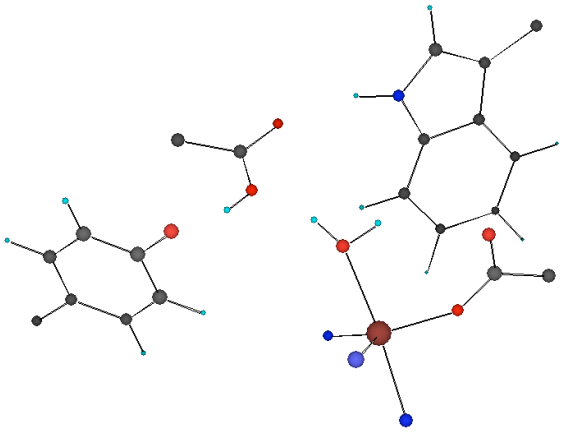

Q69E Fe^{2+}SOD: Coord H_2O, Glu69H, Tyr34$^-$

INPUT GEOMETRY

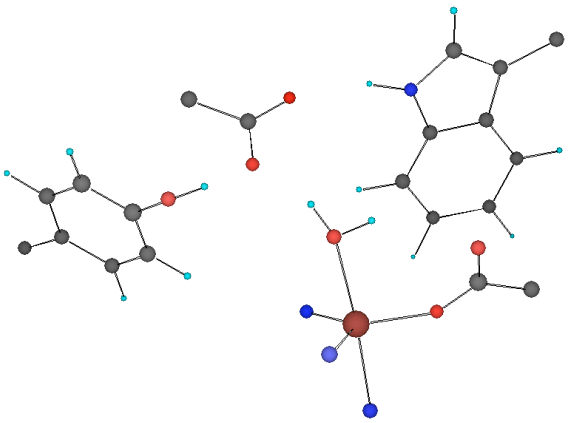

OPTIMIZED GEOMETRY

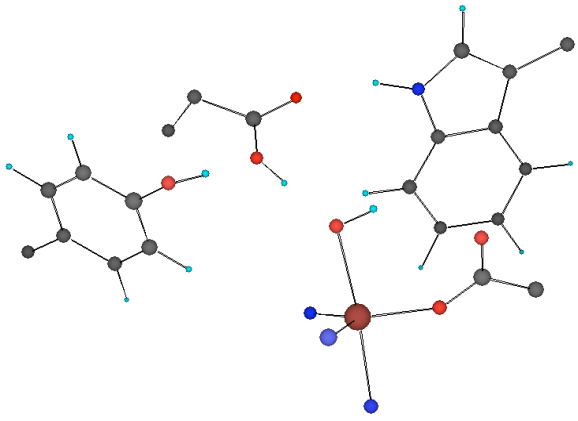

Q69E Fe^{2+}SOD: Coord OH^-, Glu69H, Tyr34H

INPUT GEOMETRY

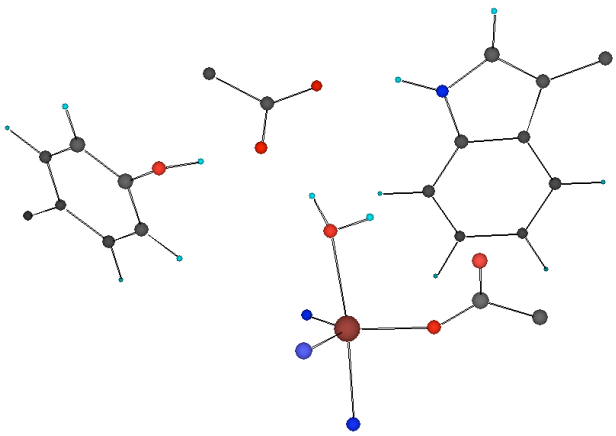

OPTIMIZED GEOMETRY

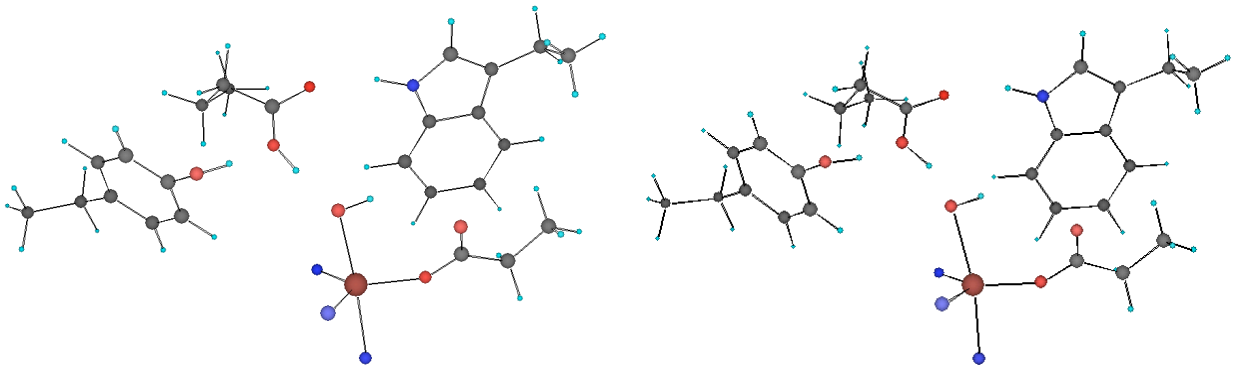

Q69E Fe^{2+}SOD: Coord OH^-, Glu69H**,** Tyr34H

INPUT GEOMETRY RESTRAINED OPTIMIZATION GEOMETRY

Figure S4: Starting and optimized structures of Q69E-Fe^{2+}SOD active sites addressed by calculations. Comparison of the top three pairs of optimized structures shows that of Tyr34, coordinated solvent and Glu69, Glu69 is predicted by calculation to be deprotonated. If another group initially lacks a proton and Glu69 possesses one, calculations document proton transfer. In order to evaluate the effect of this internal proton transfer, a partial optimization was performed, in which proton transfer from Glu69 was prevented (bottom row, and please see Table S3).

References

1. Barik, S. *Methods in Molecular Biology* **1996,** *67*, 173-182.
2. Carlioz, A.; Touati, D. *EMBO J.* **1986,** *5*, 623-630.
3. Sorkin, D. L.; Miller, A.-F. *Biochemistry* **1997,** *36*, (*16*), 4916-4924.
4. Slykhouse, T. O.; Fee, J. A. *J. Biological Chem.* **1976,** *251*, 5472-5477.